Construction and Building Materials 384 (2023) 131009

Contents lists available at ScienceDirect

Construction and Building Materials

journal homepage: www.elsevier.com/locate/conbuildmat

Def-related expansion in concrete samples and blocks with nano-sio$_2$

Mariana O.G.P. Bragança [a], Nicole P. Hasparyk [b], Kleber F. Portella [a,*], Bruna Gomes Dias [a], Luciana A. Farias [c], Jeferson L. Bronholo [a], Selmo C. Kuperman [d]

[a] Instituto de Tecnologia para o Desenvolvimento (Lactec), PO Box 19.067, CEP: 81531-980, Curitiba, Paraná, Brazil
[b] FURNAS Centrais Elétricas S. A., Rodovia BR 153, km 510, Goiânia, CEP 74993-600, Brazil
[c] Rheoworks, Rua S6, 1070, Quadras 21 Lote 05, CEP 74823-470 Goiânia, Brazil
[d] DESEK, Av. Nove de Julho, 3229, São Paulo, SP 01407-00, Brazil

ARTICLE INFO

Keywords:
DEF
Expansions
Nano-SiO_2
Concrete
Block

ABSTRACT

Constancy is necessary in finding strategies for enhancing the lifetime of concrete structures, through preventing expansive chemical reactions. Research has been published regarding the use of SCMs in DEF expansions trials. Nevertheless, there is little research involving DEF focused on incorporating nanomaterials into the cement matrix. Thus, the aim of this investigation was to evaluate the potential of DEF mitigation using nano-SiO_2. Concrete blocks and laboratory specimens were tested and as a result, a high level of DEF expansions in concrete was observed, with and without nanomaterials, noting that nanosilica was not effective in mitigating DEF.

1. Introduction

Delayed ettringite formation (DEF) is an expansive phenomenon that involves internal sulfate attack that can occur when high temperatures are reached in the concrete during cement hydration at early age. In general, temperatures between 60 and 65 °C, or even higher, can lead to some DEF risks, depending on the cement composition, the mix proportioning, and the environment.

According to some references [1,2], under high temperatures, the development of Aft phases (ettringite) in fresh concrete is unstable, presenting unexpected formations. In this condition, sulfate salts remain available in the pore solution and are suitable to react with other elements of the cement paste. Moreover, these salts can be physically adsorbed onto C-S-H, over time, to form delayed ettringite [3]. The expansions occur due to the development of DEF crystals, as shown by the theory proposed by Cohen, which states that swelling is due to water absorption [3]. Currently, there is no standardization for lab test methods to evaluate potential DEF. However, research on using new materials is constantly in evidence regarding a proper material to mitigate DEF expansion, aside from pozzolanic mineral admixtures already known.

For Giannini et al. [4], the stiffness and plastic deformation indexes, SDI and PDI, respectively, obtained from the stiffness damage test (SDT), provide information to evaluate distress caused by DEF. Similarly, these tests were carried out to assess damage caused by alkali silica reaction (ASR), whose relationship of expansion results remained almost linear to the expansion values from about 0.40%. For this test method (SDT), some important parameters were established, besides the specimen preparation, such as performing 5 repeating cycles of loading–unloading at a speed of 0.1 MPa.s^{-1}, up to a maximum of 10 MPa (limited to about 40% of the compressive strength of the specimen, as it is a non-destructive method).

Newer strategies have been developed to enhance concrete structure lifetime which aim to interrupt, or even prevent, some chemical

Abbreviations: AFM, atomic force microscope; AMBT, accelerated mortar bar test; ANOVA, analysis of variance; ASR, alkali silica reaction (ASR); B, block; BNS, concrete blocks prepared with NS at 1.0 wt% by mass of cement; C, concrete; CNF, cellulose nanofibers; CNS, concrete specimens prepared with NS at 1.0% by mass of cement; COD, crystallography open database; DEF, delayed ettringite formation; ESA, external sulfate attack; FTIR, Fourier transform infrared; GO, graphene oxide; GObm, graphene oxide ball-milled; ISA, internal sulfate attack; ITZ, interfacial transition zone; NS, nanosilica; OPCordinary Portland cement, OPC; PCE, polycarboxylate chemical admixture (PCE); PDI, plastic deformation indexes; RCA, recycled concrete aggregate (RCA).; SCMs, supplementary cementing materials; SDI, stiffness deformation index; SDT, stiffness damage test; SEM-FEG/EDS, scanning electron microscope-field emission gun type with energy-dispersive X-ray spectroscopy; XRD, X-ray diffractometry.

* Corresponding author.
E-mail addresses: mariana.portella@lactec.com.br (M.O.G.P. Bragança), nicole@furnas.com.br (N.P. Hasparyk), portella@lactec.org.br (K.F. Portella), bruna.dias@lactec.com.br (B. Gomes Dias), luciana.farias@rheoworks.eng.br (L.A. Farias), jeferson.luiz@lactec.com.br (J.L. Bronholo), selmo@desek.com.br (S.C. Kuperman).

https://doi.org/10.1016/j.conbuildmat.2023.131009
Received 27 September 2022; Received in revised form 6 March 2023; Accepted 8 March 2023

reactions, such as external and internal sulfate attack (ESA and ISA). Thus, further studies on cement composites with nanomaterials, such as silicon dioxide, magnetite, graphene, cellulose nanofiber, among others are currently being researched [5–8].

Cellulose nanofibers (CNF) used in Portland cement composites to reduce ESA, with its consequent expansion were evaluated. For studies, four types of binders were selected, as follows: ordinary Portland cement, OPC; sulfate-resistant cement; high-early strength cement; and a blended Portland cement, containing 30% fly ash. The CNF content was up to 0.5% in volume fraction [5]. An accelerated ESA test was performed in the specimens prepared with the CNF, for 12 weeks. They presented reduced sulfate penetration and stability in compressive strength results throughout the period under sulfate exposure. Additionally, a reduction was verified in ettringite formation as well as refinement in pore-size and lower expansions values [5].

Devi and Kham (2020) [6] studied the use of the graphene oxide (GO) and graphene oxide ball-milled (GObm) as admixture and evaluated their performance through ESA and accelerated carbonation tests. Therefore, six concrete mixes were prepared with 0.05% and 0.1% addition by weight of binders (OPC) and with recycled concrete aggregate (RCA). Although some mixes presented improvement in sulfate attack resistance and reduced depth of carbonation, both with GO and GObm in comparison to the reference mix, containing only RCA (100%), the microstructural analyses indicated excessive ettringite and gypsum formation during the period in which the concrete was exposed to sodium sulfate solution, in which the mass gain and the decrease in compressive strength results could be assessed.

Nowadays, nanosilica is a material widely studied as concrete admixture. Mortars with nanosilica, whose performance in sulfate resistance was evaluated when subjected to ESA in 5% Na_2SO_4 solution exposition, considering the range of 0 to 5 wt% replacement of cement, were submitted to microstructural analysis combined with mass loss, linear expansion and strength loss. The results indicated pore-size refinement and a reduction in its connectivity, associated with the use of the nano admixture. It was reflected in enhanced sulfate resistance proportional to the selected contents. Moreover, it was verified that the coarser nano silica the better its behavior, and in particular with particle size of 10 nm, on average [7].

The nanomaterials characteristics were also considered for mitigating ESA, chloride attack and their corrosive effects in reinforced concrete. Studies on Portland cement mortars prepared with ternary mixes, involving fly ash, metakaolin, slag with nano admixtures, nano silica, nano titania and nano alumina have been presented by some researchers. The results indicated that composites containing nano admixtures (at 5% content, with respect to the weight of binder) enhanced durability and corrosion resistance (tested for 90 days) and also improved the microstructure [8].

Other studies conducted using some nanomaterials as admixture in mortars and concretes to enhance their characteristics are being developed by other research [9–11]. Use of nano silica particles in 1.5% content (with respect to the weight of binder) added to lime and lime-pozzolan pastes was correlated with a decrease in macro porosity and an improvement of compressive strength. This could be due to the strong effect on pozzolanic reactions that occur with this nanomaterial [9]. In one of the most recent review papers [10], the benefits of this nanomaterial in concrete, both fresh and hardened, were also summarized. In general, the studies indicated that the use of nano silica, in different proportions, were related to the increase of mechanical properties (such as compressive, tensile, and flexural strength, and elasticity modulus) and with enhanced durability aspects, with the reduction of structural micropores. Also, the analyzed researches indicated an environmental perspective in reducing the consumption of cement, which releases CO_2 that is responsible for the global warming [10]. Used in a binary mix of 1 to 5% of the cement weight, with nano magnetite, nano silica also had an important role in concrete microstructure and in mechanical and durability properties. According to the research, there is a relation with an enhancement of the Young's modulus, the nuclei for the C-S-H phase formation and the changes in the cement gel structure, evaluated by atomic force microscope (AFM) and nanoindentation [11].

Although studies are available conducted to verify the performance of nano admixture in enhancing the mechanical properties of cement composites, including in relation to their external sulfate resistance by the exposition of samples in aggressive solutions of Na_2SO_4 (ESA), there is a gap considering these nanomaterials for mitigating expansions from an ISA, such as DEF. The research presented herein was aimed at evaluating nano-SiO_2 and its potential to mitigate DEF-induced expansion and negative consequences on concrete properties.

2. Experimental methodology

2.1. Materials

2.1.1. Cement

The high-early strength Portland cement (Brazilian cement type CPV ARI - similar to ASTM cement type III) considered in the study presents the following chemical and physical compositions, according to Table 1.

2.1.2. Aggregates

The coarse aggregate used in the mixtures was an ASR innocuous material, selected from a granitic rock and classified as granite, with maximum dimension size of 19 mm. Field registers as well as the lab tests performed by AMBT [12,13] indicated no potential ASR. The main minerals in the aggregate are alkaline feldspars 40%; plagioclase 25%; quartz 20%; biotite 10% and other minor minerals such as sericite, hornblende, opaque, chlorite and zircon, up to 5%. Fine aggregates were used, mainly composed of quartz grains and some schist fragments. It has maximum dimension size of 4.75 mm and fineness modulus of 2.64. According to AMBT tests, these materials were also considered potentially innocuous to ASR [12,13].

2.1.3. Nano-SiO_2

Intending to evaluate their potential in mitigating DEF, a commercial nano-SiO_2 (NS) was used. NS was applied in a colloidal form, with 30% of solid content, 305 m^2/g average surface area and pH 10.5. The nanomaterial was previously characterized by SEM-FEG/EDS, as shown in Fig. 1. The NS was also evaluated using Fourier transform infrared spectrophotometry (FTIR). The spectrum acquired was over the 5000–400 cm^{-1} range with a 4 cm^{-1} resolution and the samples were prepared in KBr pellets (Fig. 1). Additionally, it was analyzed by X-ray diffraction technic, XRD, using polycrystalline powder samples with Cu-Kα radiation, a wavelength λ of 1.5418 Å, a 2θ scanning range between 0° and 70°, a 40 kV voltage, a 25-mA current, a 0.02° pass and a 0.1p/s pass speed. The chemical phases were identified by the Crystallography Open Database, COD.

According to SEM (Fig. 1a), NS particles feature an angular morphology, in conglomerations of different sizes. Elementary

Table 1
Chemical (% by mass) and physical characteristics of cement.

SiO_2	Al_2O_3	Fe_2O_3	CaO	MgO	Total alkalis		
					Na_2O	K_2O	Na_2Oeq
17.6	4.00	3.50	63.40	3.10	0.20	0.80	0.73
Soluble alkalis			**Loss on ignition**	**SO_3**	**Free lime**	**Insoluble residue**	
Na_2O	**K_2O**	**Na_2Oeq**					
0.20	0.70	0.66	3.64	3.00	0.81	3.32	
Specific Gravity (g/cm^3)		**Blaine Fineness (cm^2/g)**		**Autoclave expansion (%)**		**Initial Setting time (min)**	
3.10		4.72		0.00		185	
Final Setting time (min)		**Compressive Strength at 3 days (MPa)**		**Compressive Strength at 7 days (MPa)**		**Compressive Strength at 28 days (MPa)**	
350		32.30		35.10		42.50	

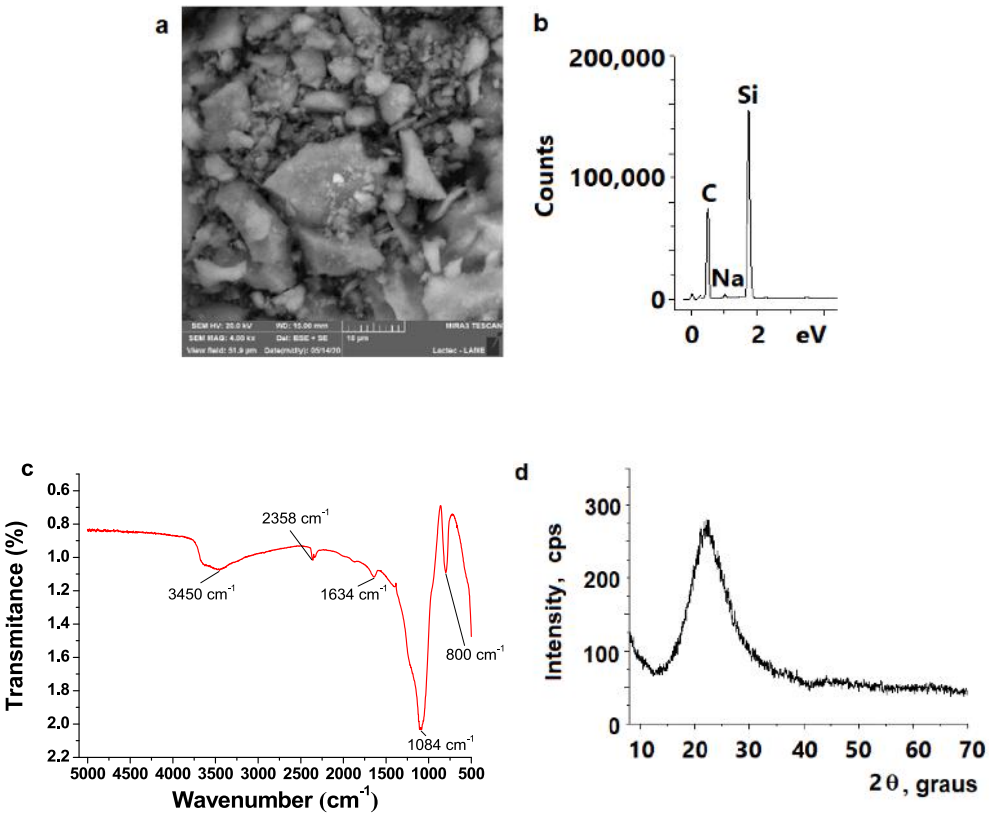

Fig. 1. NS characterization by: a) SEM-FEG micrography; b) EDS spectra; c) FTIR; and d) XRD.

composition by EDS indicated basically Si, O and Na, as previously provided by the manufacturer. FTIR analyses (Fig. 1c) indicated five characteristic bonds for NS: a wide one, at 3,450 cm^{-1}, that correspond to O-H and SiO-H stretching vibrations; a little bond, at 2,358 cm^{-1}, relative to Si-H_3 stretching or correspondent to the vibration of atmospheric CO_2; another, at 1,639 cm^{-1}, corresponded to v_2-H_2O; and the last two, at 1,084 cm^{-1} and 800 cm^{-1}, that were associated with Si-O asymmetric and symmetric stretching, respectively [11–14]. The XRD (Fig. 1e) spectrum presented only one amorphous halo at an angle correspondent to the silica chemical phase (S).

2.2. Rheological studies of the cement paste with NS

A rheological study was carried out with different nanomaterial contents to visualize the behavior of five mixtures and to define the final composition to be used in concrete specimens and blocks.

The cement pastes with the nano-SiO_2 were established in the laboratory considering the best rheological conditions, thus the nano rate ranged from 0.5% to 2.0% and the results were compared to a reference, without nanomaterial, to evaluate their performance and select the best condition.

In the study, two experimental conditions were considered: the first with cement Brazilian type CP V; the other with the addition of colloidal NS, with 30 wt% in solids, pH 10.0 and 305 m^2/g of surface area, with solid proportion of 1 wt% in relation to the cement mass. The water cement ratio considered for all mixtures was equal to 0.46, besides 0.1 wt% lignosulfonate chemical admixture and different rates of polycarboxylate chemical admixture (PCE) to reach the flow value of (100 ± 10) mm in the mini slump apparatus. The cement pastes were stirred in a mechanical mixer for 1 min at 1,250 rpm and 3 min at 2,500 rpm.

The rheological study was conducted, adopting the flow regime of parallel plates with dimensions of 40 mm in diameter and 1 mm gap, at a temperature of 23 °C. For this study, the test procedure considered for the flow involved three cycles of acceleration and deceleration, resulting in six flow curves (Flow1 to Flow6), as shown in Fig. 2. The duration of each cycle was 120 s (60 s for each flow), resulting in a total test time of 6 min for each sample. To analyze the rheological behavior, only flows 3 (breakdown, represented in the graph by a line with filled triangles) and 4 (build-up, represented in the graph by a line with empty triangles) of the adopted procedure were considered (Fig. 2).

As can be seen in Fig. 2, all the cement pastes with cement Brazilian type CP V (High early strength cement) tended to present rheopectic behavior, given by their hysteresis area. However, even though all combinations present the same behavior, the impairment in viscosity is reduced by adding PCE. So, even maintaining the 0.1% content of lignosulfonate chemical admixture for all combinations, it was necessary to add the PCE to enable the desired mixture flow to be achieved and to evaluate the behavior of mixtures with NS contents above 1.0%.

The best behavior indicated by the rheological study was observed in the mixture with 1.0% NS, even with the rheopectic tendency. Although the paste with 2.0% NS had a buildup cycle performing over the breakdown cycle, its behavior was like that observed in the paste with 0.5% NS, with an increase in viscosity even with a high PCE admixture content. The rheological behavior showed an improvement in performance up to the incorporation of 1.0% of NS, presenting potential difficulties in the mixture workability, even under the same flow, above NS content of 1.5%. According to the viscosity graph, this becomes more effective when observing the reach of lower viscosity at the 1.0% content, followed by the 1.5% content, after which the increase in cement paste viscosity becomes more pronounced, even with the use of PCE to improve dispersion of components.

2.3. Composites, environmental exposure, and tests

2.3.1. Concrete samples

The concrete reference mixtures for both cylindrical C and block B

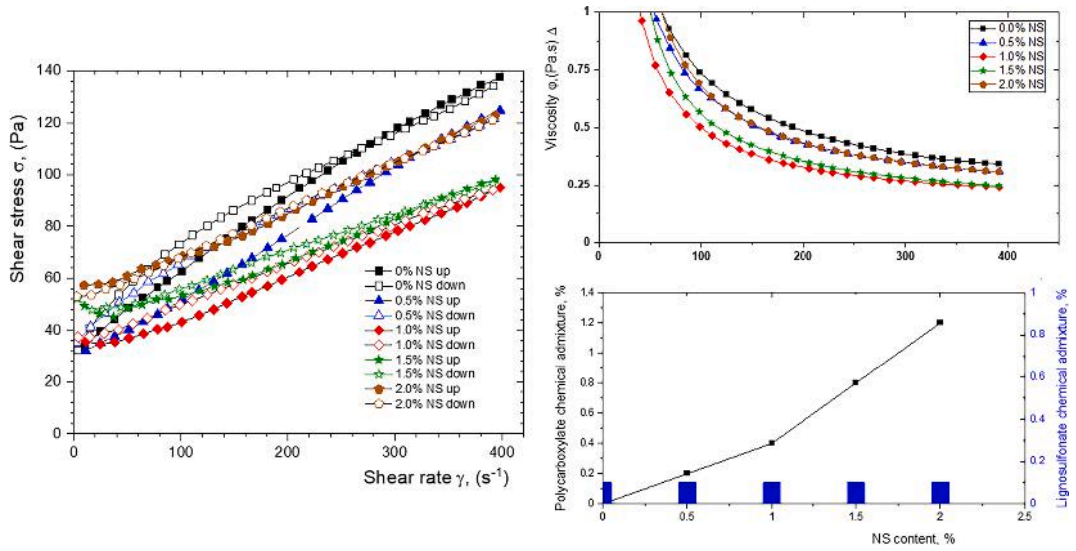

Fig. 2. Flow curves and rheological behavior of six different mixes of cement paste with and without NS.

samples were produced, as follows: 1:1.6:1.8:0.46 (cement: sand: coarse aggregate: w/c ratio) with cement content of 471 kg/m^3. It was considered the use of 0.22% lignosulfonate-based chemical admixture and 0.18% viscosity-modifying and superplasticizer (PCE) chemical admixture, the latter used to adjust the final consistency.

Specimens were prepared with NS at 1.0 wt% by mass of cement (CNS and BNS). Additionally, in all the mixtures an extra NaOH addition was necessary in order to achieve a Na_2O_{eq} total content of 1%.

Concrete prisms (75 × 75 × 285) mm were cast in the laboratory according to a reference concrete mix design for monitoring expansion over time and corresponded to a case of concrete massive element that achieved temperatures above 80 °C at a site, from a hydroelectric power plant, thus, exhibiting thermal history in the field due to hydration heat.

Cylindrical specimens were also cast [(100 × 200) mm] to perform mechanical tests at specific ages. They were evaluated in accordance with the Brazilian standards (ABNT NBR), as: i) compressive strength test, according to NBR 5739 [14]; and ii) compressive elasticity modulus, according to NBR 8522 [15], both performed after 3, 7, 28, 91, 180, 270, 360 and 450 days of heat treatment. All the obtained results were statistically evaluated using the ANOVA and Tukey tests.

2.3.2. Block samples

Concrete was placed inside wooden cube-shaped molds with 80 cm sides, coated internally with 15 cm of Styrofoam to reach a semi-adiabatic curing temperature, above 65 °C, minimum, to induce DEF. The shape and dimensions of the mold, as well as the built-in deformation and thermal sensors, were illustrated in Fig. 3. For this purpose, up to 4 thermocouples, a Carlson type strain meter and a rod extensometer were used internally in each block, and their data electronically collected online and in-situ during the 450 days of exposure to the natural environment, in Curitiba, Paraná, southern Brazil (25°26′41″S-49°14′06″W). The average local temperature conditions (statistically evaluated over the last 30 years) were, in the summer, about (17.20 ± 0.96) °C, with maximum averages of (25.00 ± 0.00) °C and rainfall rates of (179.75 ± 36.59).) mm; in autumn, around (13.50 ± 3.11) °C, with maximum averages of (21.75 ± 2.75) °C and rainfall of (106.00 ± 22.58) mm; in winter, around (10.50 ± 1.00) °C, with maximum averages of (19.25 ± 0.96) °C and rainfall of (106.25 ± 25.08) mm; and in spring, in the order of (14.25 ± 1.71) °C, with maximum averages of (22.50 ± 2.08) °C and rainfall indices of (148.00 ± 13.14) mm, respectively [16]. It was important to analyze these exposure conditions to verify the effect of thermal and humidity cycles.

During the exposure time of the blocks in the field, in addition to the strain and temperature measurements, non-destructive electrical resistivity tests were carried out, using the Wenner probe method, in Resipod type equipment, (UNE 83998–2 (2012) [17]), visual inspection and ultrasound wave propagation speed, direct and semi-direct method, with a 54 kHz transducer and methodological recommendations from the ABNT NBR (8802) [18] standard, Aggelis et al. (2010) [19] and Hasparyk (2005) [20], to assess homogeneity, the presence of internal

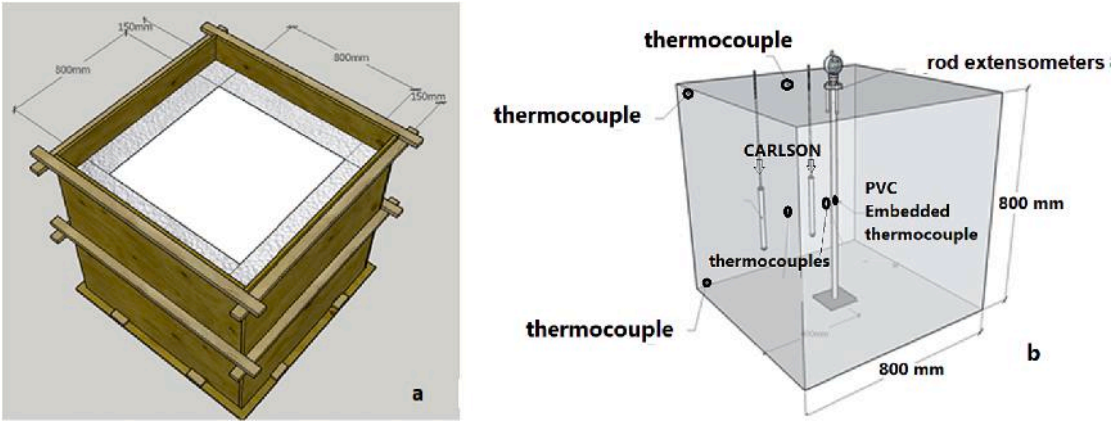

Fig. 3. Schematic drawings of the mold and concrete blocks built for the DEF formation test, in a natural environment aging.

flaws, among other pathological manifestations.

Concrete cores were also drilled from different areas of the blocks, with diameters up to 15 mm for the mechanical, physical–chemical, and microstructural characterization of concrete under natural aging.

The samples were encoded, and their characteristics were summarized in Table 2.

After casting, all concrete specimens were subjected to a specific heat treatment for DEF, according to Fig. 4. Immediately after thermal treatment, the specimens were submerged in a water container and stored at 38 °C over time, up to 450 days.

The concrete blocks (BNS and B) were exposed to a natural semi-adiabatic heat treatment due to the temperature rise during cement hydration over time. The thermal treatments were equivalent to that shown in Fig. 4, knowing that: 1- concrete casting; beginning of temperature ramp (2); holding (3); cooling (4); and maintaining at room temperature (5), without immersion in water. The results of the heat treatments of the samples could be seen in Fig. 5. The experimental results showed the effectiveness of the thermal conditioning system, during the curing of the block samples for DEF, reaching levels of 95.2 to 61.9 °C and 89.9 to 59.6 °C, in BNS and in B, respectively. Thus, the samples had achieved temperatures above 65 °C, for a minimum period of 6 and 5.6 days, respectively.

Once the mechanical tests were performed, concrete fragments from the specimens and blocks were collected for microstructural analyses using SEM/EDS. Fracture surface analyses were carried out for all specimens using a BSE/SE paired detector, in a proportion of 70/30.

Due to the small dimensions of the blocks and to keep them in natural exposure for as long as possible, it was decided to remove a few samples of concrete for the destructive tests in the period, with exceptional removal of specimens when visible damage occurred.

3. Results and discussion

3.1. Expansion tests

The expansions of the specimens C, CNS, B and BNS are shown in Fig. 6. Under the same test conditions, samples C and CNS aged in a controlled aqueous environment at 38 °C, with more probability of expansion, of 0.59% and 0.41%, respectively. BNS samples presented 0.12%, showing the peculiar behavior of the material when exposed to natural climatic conditions, especially when lower temperatures and humidity levels were reached, in the same period. However, in both situations greater expansions were identified for samples containing nano-SiO_2 (CNS and BNS). For both cases, it could be considered that the pozzolanic activity of the admixture was not very effective, that is, the solution of capturing Ca ions in the pores and voids was not enough to enhance the microstructure of the concretes, reducing the water access and, consequently, reducing the expansive parallel reactions of late ettringite. As studied for Atahan and Dikme [23], the formation of ettringite is dependent of some factors, such as the disponible of the main reaction products: monosulfate, gypsum and, specially, water.

Table 2
Type of mixes, condition of treatments and exposure environments.

Sample identification		Age	Exposure	Cement with no admixture	Cement + NS
Concrete specimens cast at lab	C CNS	(up to) 450 days under lab conditions	38 °C; in water	X –	X
Blocks and concrete cores	B BNS	(up to) 450 days under natural environment	External environment	X –	X

The expansions of concretes with NS could be a consequence of the small amount of nano-SiO2 used (1 wt% of cement weight) and to the nanomaterial tending to capture more hydration water and few CH [24]. The possibility that its content was insufficient during the setting and curing of the concrete could have been prominent, creating suitable sites (increases in internal voids) for DEF to develop. Comparing the obtained data with the previous research developed by Atahan and Dikme [23], which reported enhanced results for the expansive behavior of mortars containing NS subjected to ISA, it could corroborate this hypothesis. In this paper, it was used three different amounts of NS, 2%, 4% and 6% and the expansive behavior was lesser with higher addition mixes. The authors also concluded the 4% NS mix was safe, considering the limit of 0.1% of expansion. Such an occurrence was observed even using the optimal conditions of mixtures and their rheological results. Senff et al. [24] studied mortars with contents of nano-SiO_2 from 0 to 7 wt% and observed that structures formed quickly during rheological measurements, with changes in the particle friction and free water parameters, showing high initial and final torque values, with low plasticity, between 120 and 135 min of tests, attributing changes in the evolution of cement hydration.

In larger field structures, such effects or damage can be more pronounced, as verified in BNS block structures with nano-SiO_2 (Fig. 7). In this case, the external damage was visually more expressive in terms of cracking, already occurring in expansion values around 0.04% at about 280 days, lower, therefore, than reported in the literature for occurrences for DEF [25]. According to Brunetaud et al. 2008 [25], up to 0.04% of expansion no macro symptoms or defects are observed. This same threshold (0.04%) is established in the Brazilian technical procedure to indicate a concrete's potential for DEF [21].

3.2. Mechanical properties

The compressive strength data from concrete specimens are shown in Fig. 8. In general, specimens showed an evolution in performance over time, and up to 3 months. However, NS samples (CNS) did not maintain evolution at higher ages, especially after 6 months, with drops around 22% at 450 days. For C samples, the decrease for the same period was about 14%. The statistical analysis showed there was no significant difference between the two mixtures, for the concretes, over the exposure time. Even though, by the Tukey test, differences were detected between the C and CNS concretes, respectively.

The compressive strength results of the BNS core samples, drilled from the concrete block, presented average values close to those of the respective specimens (CNS) cast in the laboratory, in the considered time interval (100–150 days), of (36.30 ± 3.18) MPa, compared to (43.17 ± 2.06) MPa, respectively. On the other hand, B, presented a result lower than that (about 38%) of C, of (41.32 ± 2.31) MPa, compared to (25.70 ± 0.78) MPa, respectively. This may be a consequence of the controlled conditions of exposure of sample C, in an aqueous environment and at a constant temperature of 38 °C, in the laboratory, since no visual damage was detected in the block in the respective period, even using the non-destructive tests that will be discussed later.

The modulus of elasticity for all mixes tested is shown in Fig. 9. This property has been reported as an important influence on the DEF induction process [1,25–27]. Comparing the results of the C and CNS samples, a similar behavior of the property was attributed up to about 270 days, with a constant decrease after 28 days, of about 26% (C) and 38% (CNS), up to 450 days. Between the ages of 270 and 360 days, samples with NS showed a significant drop in the values in the order of 28%, compared with 7%, but after that, both mixtures remained stabilized until 450 days.

The reduction in the elastic modulus values in the NS samples was indicative of the effect of DEF development and spreading, corroborating the morphology of the fracture surface of the material, analyzed by SEM/EDS, shown in Fig. 10.

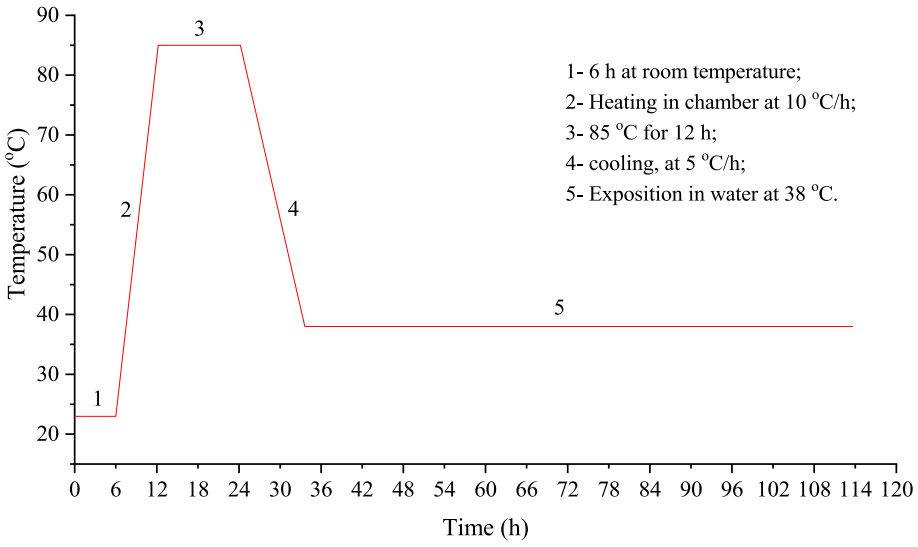

Fig. 4. General heat treatment schematic curve developed under the cylindrical samples in correspondence to that which takes place on massive elements, . adapted from [21,22]

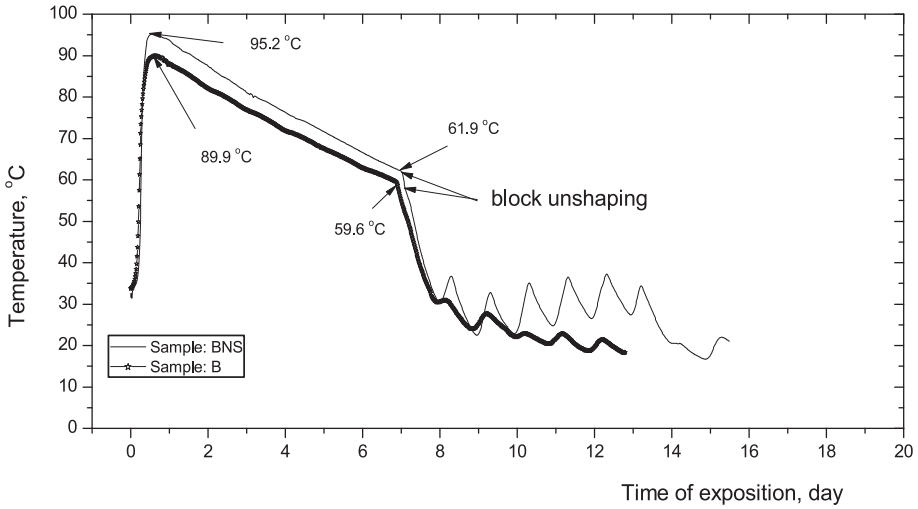

Fig. 5. Graphical presentation of the temperatures ranges of BNS and B, in the center of the block.

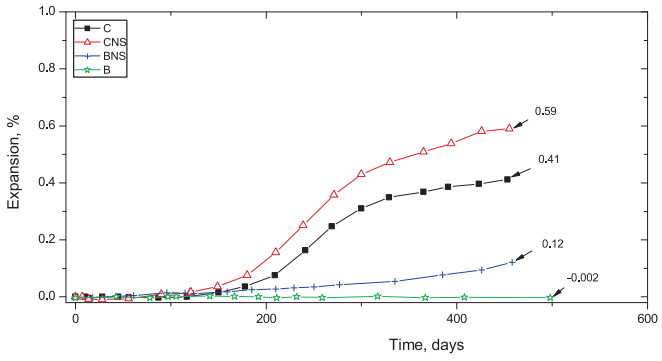

Fig. 6. Average expansions for cylindrical and block samples over time.

In the core samples extracted from the blocks, similar elastic modulus values were observed for compositions without and with NS, of (22.0 ± 3.2) GPa and (21.4 ± 0.8) GPa, respectively, at the age close to 130 days, being, on average, equivalent to those of laboratory samples. From the results, it cannot be inferred whether or not the performance of the concrete was altered in the respective control age.

3.3. Microstructural analysis

3.3.1. SEM/Eds

The microstructural analysis of the cast cylindrical concretes using SEM/EDS is shown in Fig. 10. The presence of DEF was morphologically characterized (massive or compressed form) and confirmed by EDS chemical analysis (elementary proportion Al, S and Ca), indicated with yellow dotted line. At 91 days, there was compressed ettringite at some areas in the specimen C (Fig. 10 a) and ettringite needle-like crystals filling the pores in small amounts in CNS (Fig. 10 d). After 9 months of exposure, DEF was generalized in all analyzed fragments of the specimen, while it was not very expressive in CNS, although already occupying aggregate-paste transition zones (Fig. 10 e). Furthermore, in concrete samples containing a cement with no mineral admixture, Schovanz (2019) [28] observed the extent of DEF in the cement paste and in the ITZ at 9 months, as well as ettringite deposition over aggregates and loss of bond.

At 450 days, DEF and microcracks were present and spread in both cases (with and without NS), indicated with yellow arrows in the Fig. 10

Fig. 7. Images of the BNS sample with surface cracks after one year of exposure in the natural environment.

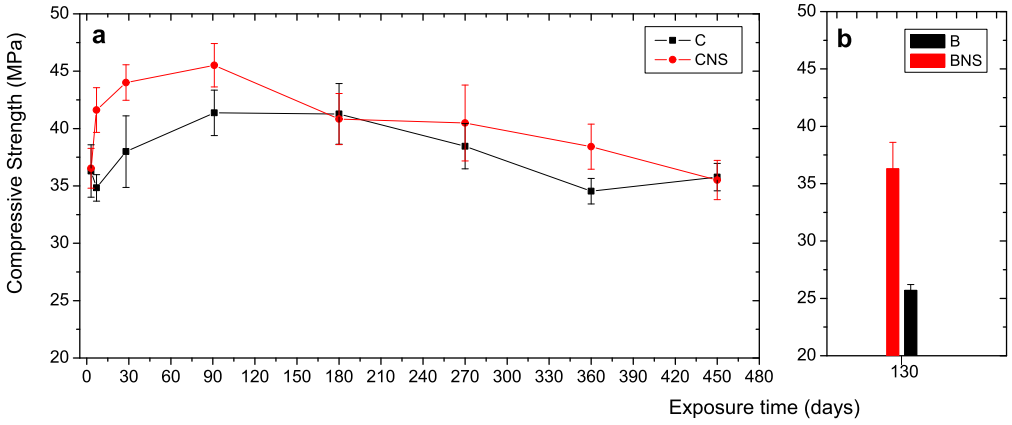

Fig. 8. Compressive strength of concrete specimens (a) C and CNS (b) samples drilled from block, B and BNS, respectively.

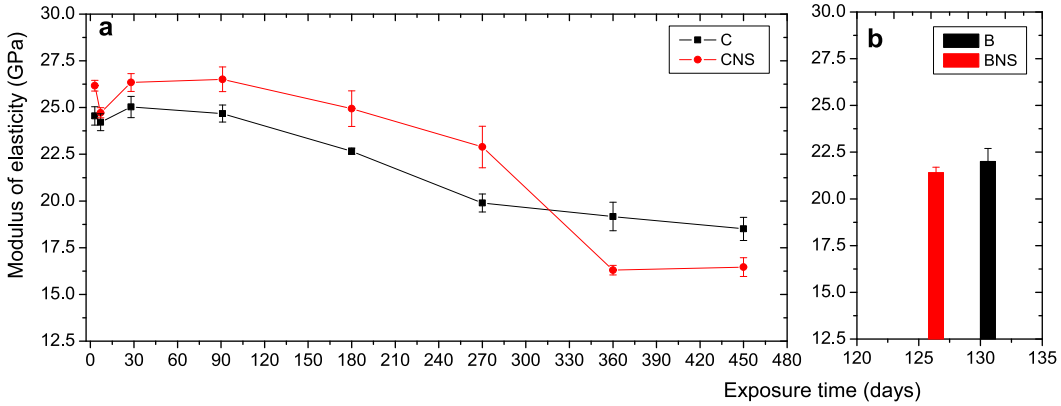

Fig. 9. Modulus of elasticity of concrete specimens (a) C and CNS and (b) drilled from block, B and BNS, respectively.

c and Fig. 10 f. Tiecher, Langoski and Hasparyk (2021) [29] reported intense microcracks, filled pores and massive ettringite in both cements paste and ITZ after 1 year in a concrete without mineral admixture. Schmalz (2018) [30] also reported a large amount of DEF in the cement matrix and in the ITZ in mortars without admixture but, in the mortar with NS, no ettringite or expansion were detected. However, this study was performed for just 90 days and, in the presence of mineral admixtures and pozzolans, the development of expansion is generally delayed (ZHUANG; SUN, 2020) [31] and further investigations must be conducted to affirm mitigative behavior. According to Silva et al. (2020) [32], this occurrence is dependent on the effectiveness, type and content of mineral admixture.

As could be seen in the micrographs shown in Fig. 11, for both concretes, the Aft crystals were formed in the cement paste as well as in the voids, and as the progress of chemical reactions tended to propagate throughout the cement matrix in the form of massive ettringite leading to intense microcracking as well, as also detected by Hasparyk et al. (2022) [33] with laboratory concrete specimens. This occurs mainly due to the lack of available areas to grow, such as free spaces; thus, crystals exert pressure promoting a fragile condition [33].

Regarding the block of concrete, the pores remained partially empty up to 365 days. Furthermore, the formation of DEF differed between B and BNS, according to the micrographs shown in Fig. 12 and Fig. 13. The intensity of crystals for BNS was more expressive in the cement matrix and both concretes contain secondary ettringite from DEF partially covering the voids.

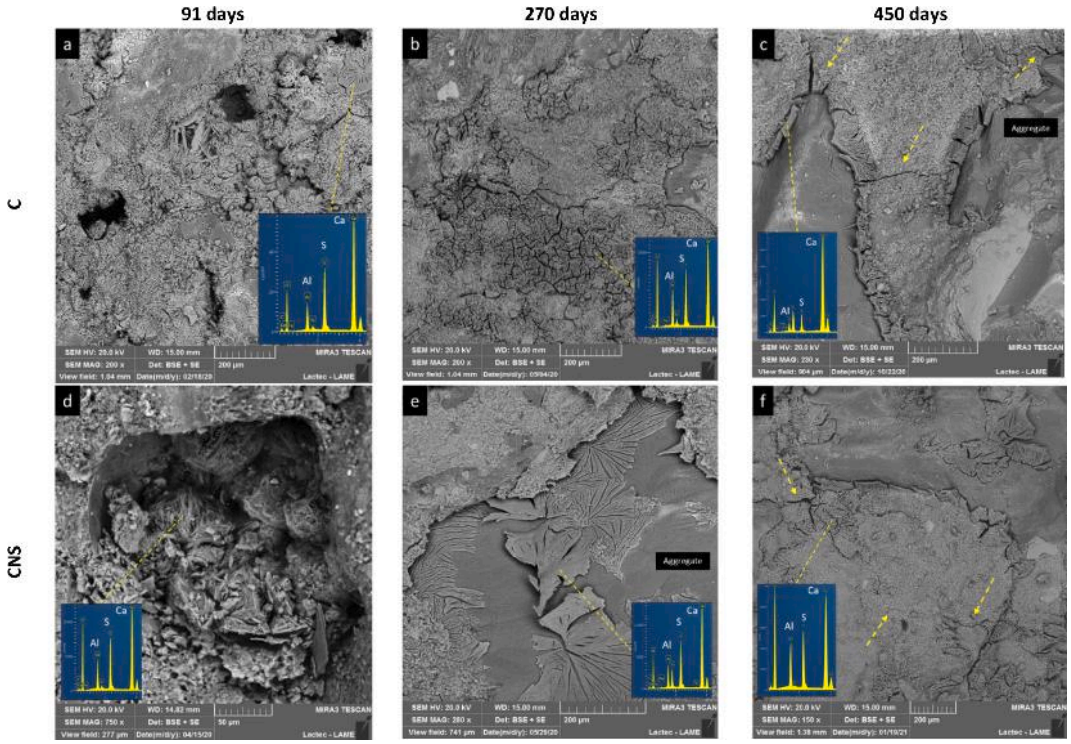

Fig. 10. SEM micrographs of concrete specimens induced to DEF: (a, b, c) C; (d, e, f) CNS.

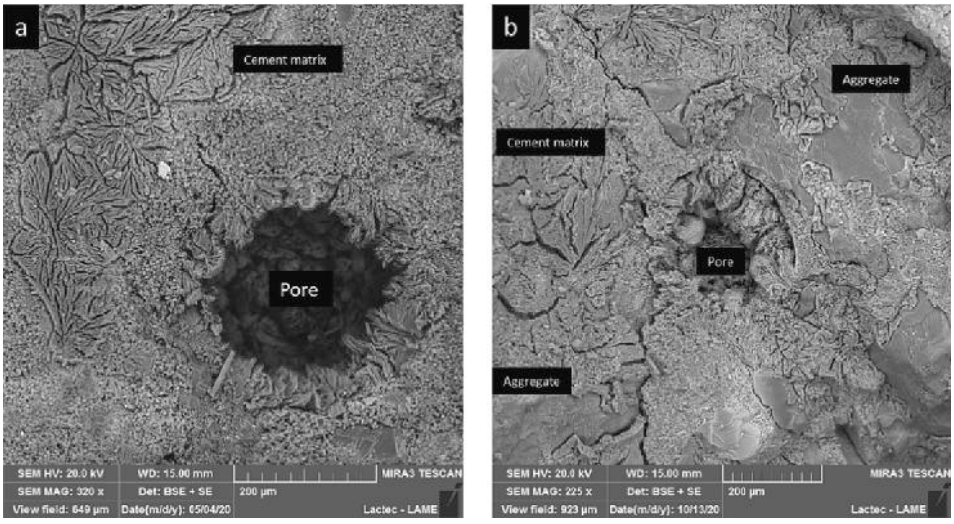

Fig. 11. SEM micrographs of concrete specimens: (a) C 270 days (b) CNS 365 days.

For sample B, typical massive DEF was only observed at 365 days (Fig. 13b). Meanwhile, before this, some intermediate phases, including calcium monosulfate, could be seen in an expressive concentration in the voids at 130 days. On the other hand, the DEF seemed more advanced for BNS since ettringite was identified in the interfacial transition zone at 130 days (Fig. 13c). After 1 year, compared to the previous control date, there was important progress in ettringite crystals to a greater extent, and microcracking (Fig. 13d).

As reported by Taylor (2001) [34], laboratory studies represent the worst-case scenario in relation to typical field concretes, such as concrete blocks, therefore expansion or cracking presented different speeds. Similarly, it can be considered that the observation of DEF also differed between samples B and C, as observed in Figs. 10 and 13, as they have different exposure environments, different sizes and variety in the availability of moisture, which was one of the factors for the occurrence of DEF.

3.3.2. XRD and DTA/TG

The results of qualitative mineralogical analysis by X-ray diffraction and the thermal analysis were shown in Fig. 14 and Fig. 15. For the concrete specimens cast in the laboratory, the presence of ettringite, portlandite, calcite and quartz were identified at the ages of 270 and 450 days.

In the concrete blocks the ettringite was evidenced in trace levels and, therefore, it was not highlighted in the X-ray diffractogram, in addition to calcite, portlandite, quartz, feldspar and mica mineral groups at the ages of 130 and 365 days. The failure to detect high levels of ettringite by XRD, despite visualization by microscopy, may be

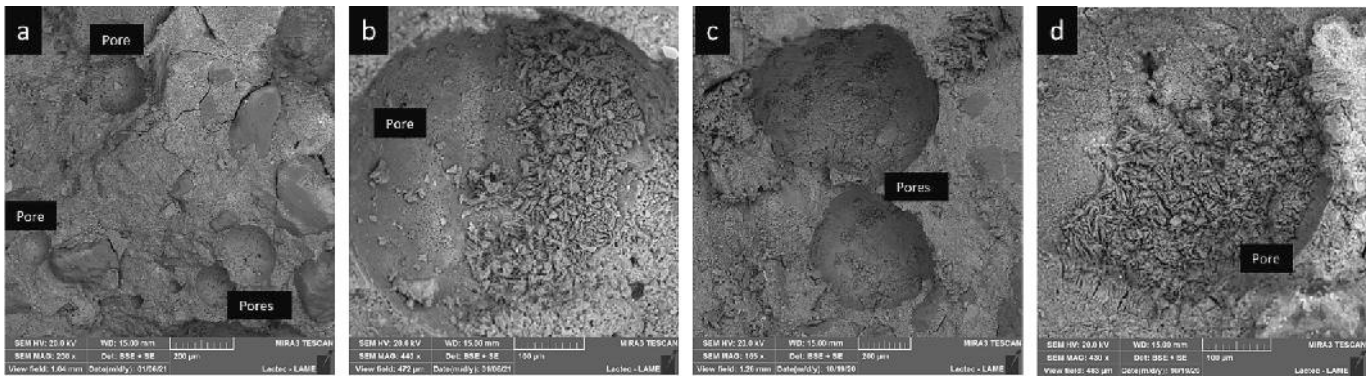

Fig. 12. Pores of concrete blocks by SEM: (a, b) B-365 days (c, d) BNS −365 days.

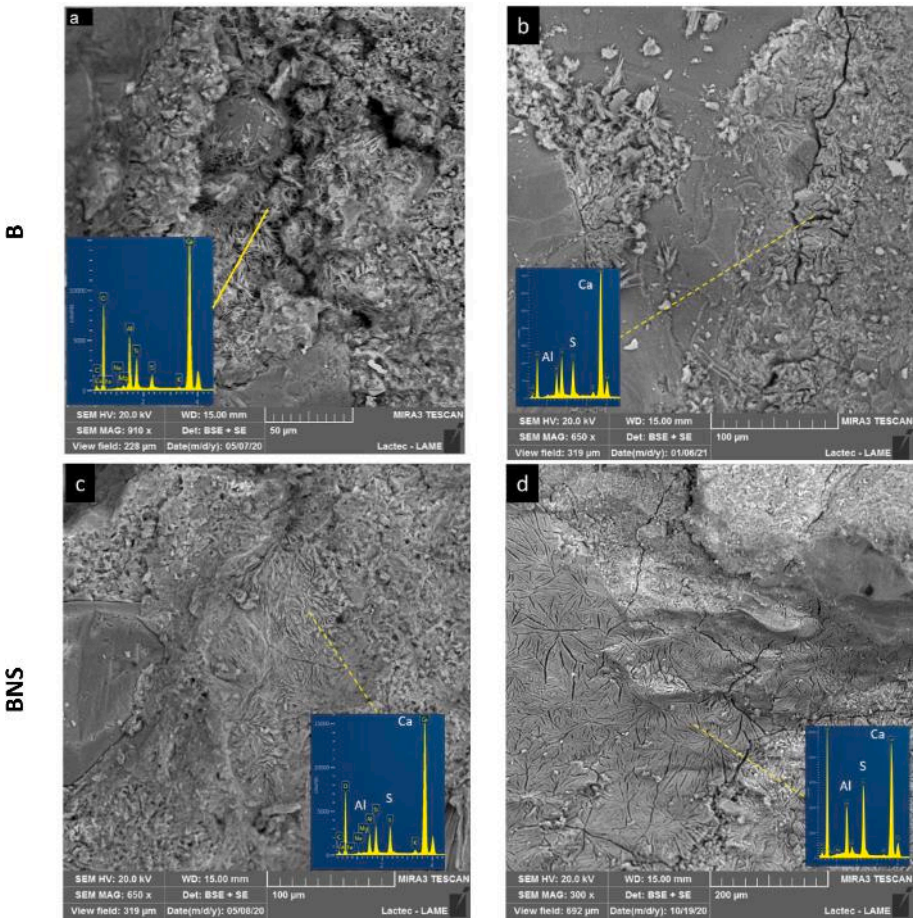

Fig 13. SEM micrographs of concrete blocks subjected to DEF. (a, b) B (c, d) BNS-DEF.

related to sample preparation, its concentration and stabilization of the crystalline structure of the molecule, among other factors related to the technique [22].

3.4. Nondestructive analysis

Based on the electrical resistivity results of the concrete specimens shown in pairs in Fig. 16, no significant changes were observed over the 450 days. However, after 250 days, the samples with NS (CNS and BNS) showed visual trends of reduction, although with similar statistical values, given the greater dispersion of the results found. This observation, however, corroborates the reduction found in the modulus of elasticity, which may be a consequence of a greater formation of DEF. The ultrasonic pulse velocity test showed no significant changes for the laboratory and field samples over the analysis period, as shown in Fig. 17.

3.5. Stiffness damage index (SDI) and the plastic deformation index (PDI)

SDT studies performed at 450 days with concretes cast in laboratory indicated a significant difference among the mixtures, according to the stress–strain curves from the five cycles applied to cylindrical specimens (Fig. 18). Both the Stiffness damage index (SDI) and the Plastic deformation Index (PDI) were higher for concrete containing NS. This behavior indicates that CNS promoted an acceleration in damage from

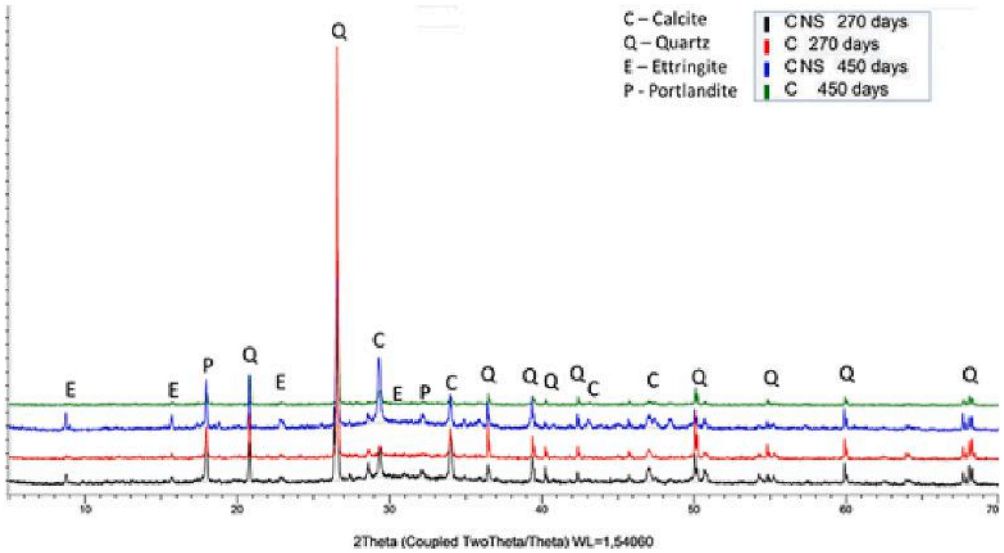

Fig. 14. XRD analyses of concretes at 270 and 450 days of ageing time, C and CNS.

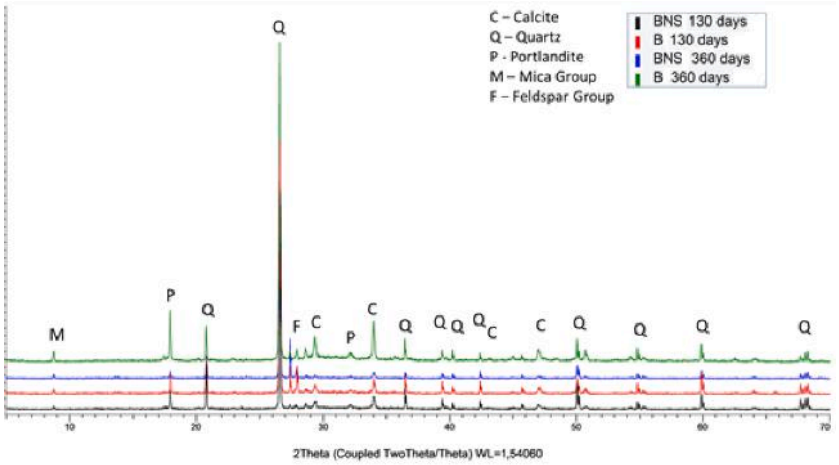

Fig.15. XRD results of concrete blocks at 130 and 365 days of ageing time, B and BNS, respectively.

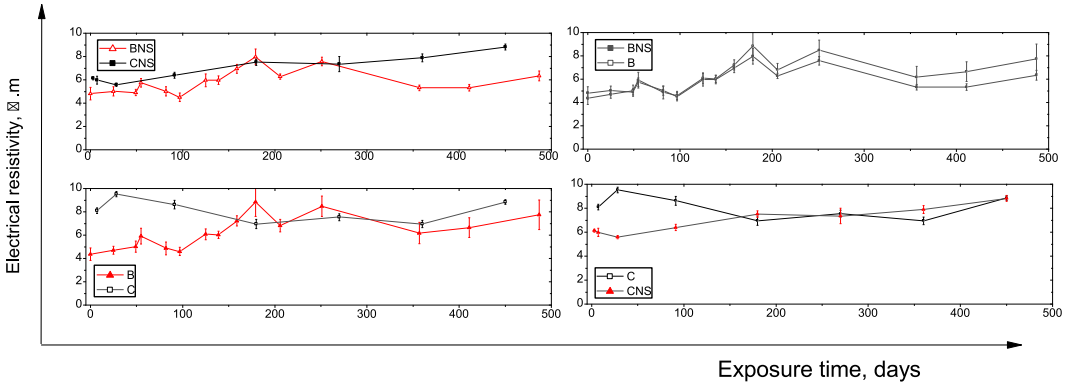

Fig. 16. Results of electrical resistivity of cylindrical and block samples, C, CNS; and B, BNS, respectively.

DEF over time, thus not mitigating the expansive process and corroborating the high level of expansions, nearly 0.60% at 450 days (SDI = 0.43 and PDI = 0.26). Reference concrete presented the following values for the same age: expansion of 0.40%, SDI = 0.27 and PDI = 0.15. Based on those data (Fig. 19), concrete with NS indicated about 50% more expansion than reference and a damage to stiffness in the order of 60% higher than reference concrete. In relation to plastic deformation capacity, the increase was much higher, and equal to 76%.

According to Giannini et al. (2018) [4], Schovanz et al. (2021) [28] and Hasparyk et al. [33], similar behavior was observed: the greater the

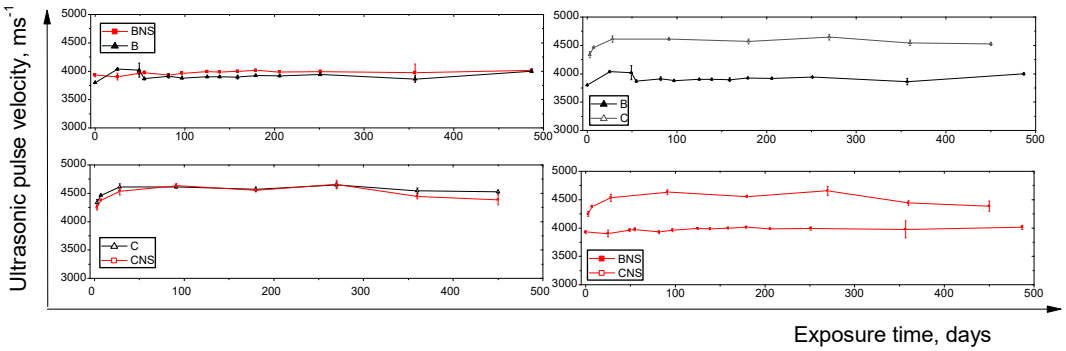

Fig. 17. Results of ultrasonic pulse velocity of cylindrical and block samples, C, CNS, and B, BNS, respectively.

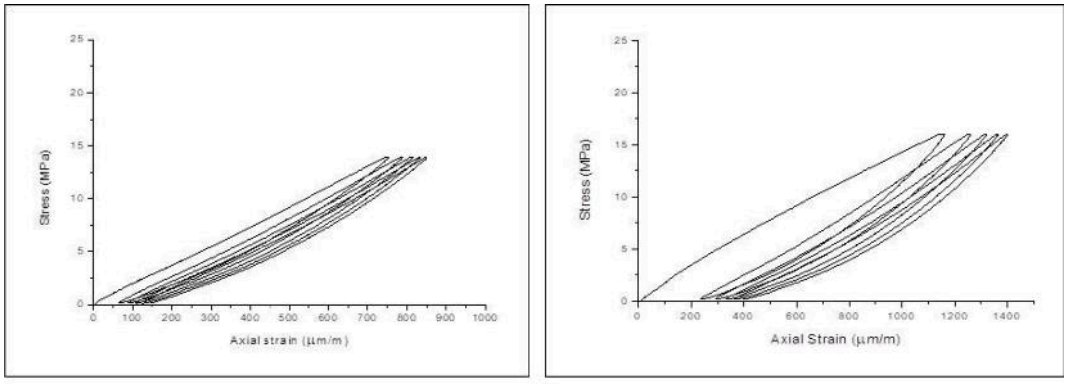

Fig. 18. Stress–strain curves from SDT: a) C; and b) CNS, respectively.

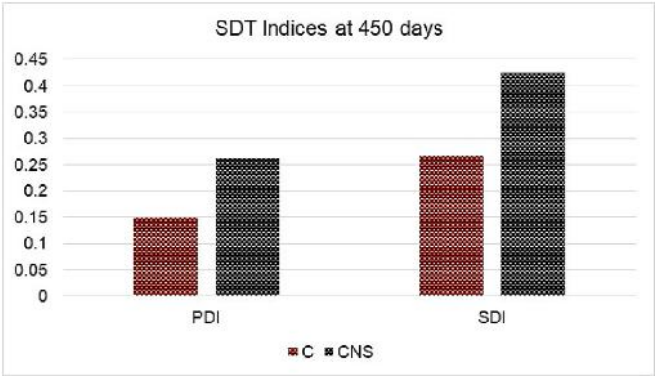

Fig. 19. SDI over time for the concrete samples, C and CNS, respectively.

expansions the higher the level of both indexes determined based on the stiffness damage test (SDI and PDI) and, thus, the global level of damage.

4. Conclusions

In this research, NS was used as nano admixture in concrete subjected to DEF induction to evaluate its performance over time. Based on the obtained results, it was concluded that NS was not effective in mitigating DEF and damage by the high temperatures for either laboratory and field tests when used in the content of 1%. This nano admixture reduced some negative consequences of DEF in the early stages, but after 3 months presented high level of expansions and negative impacts on the mechanical properties due to the intense formation of massive ettringites from the microstructure point of view. The worse performance was also attributed to some influence on the chemical process as the major water absorption by NS in fresh concrete development. This consideration must be evaluated to verify an optimum NS content and, also, ternary combinations, mainly for field structures, and their potential to reduce DEF-related problems in concrete structures. Concrete blocks with NS and exposed to environmental conditions also indicated an advanced progress of DEF at one year due to the high initial temperatures achieved, with expressive visual cracking, corroborating the behavior observed with the specimens that were cast in the laboratory and monitored over time, after induced to DEF at 85 °C.

CRediT authorship contribution statement

Mariana O.G.P. Bragança: Conceptualization, Writing – original draft, Formal analysis, Writing – review & editing, Supervision, Data curation. **Nicole P. Hasparyk:** Project administration, Conceptualization, Writing – original draft, Formal analysis, Writing – review & editing, Supervision, Data curation. **Kleber F. Portella:** Project administration, Conceptualization, Writing – original draft, Formal analysis, Writing – review & editing, Supervision, Data curation. **Bruna Gomes Dias:** Methodology. **Luciana A. Farias:** Methodology. **Jeferson L. Bronholo:** Methodology. **Selmo C. Kuperman:** Conceptualization, Writing – review & editing, Supervision, Data curation, Writing – original draft.

Declaration of Competing Interest

The authors declare that they have no known competing financial interests or personal relationships that could have appeared to influence the work reported in this paper.

Data availability

No data was used for the research described in the article.

Acknowledgements

This work was supported by ANEEL (PD 0394-1504-2015), ELETROBRAS-FURNAS, LACTEC and CNPq (Law 8010/90 - LI 15/2187214-1; LI 14/4695814-5; LI14/3410726-9; DT 302672/2016-8 and 308777/2020-4).

References

[1] M. Collepardi, A state-of-the-art review on delayed ettringite attack on concrete, Cem. Concr. Compos. 25 (2003) 401–407, https://doi.org/10.1016/S0958-9465(02)00080-X.
[2] H.F.W. Taylor, Cement chemistry, Cem. Chem. (1997), https://doi.org/10.1680/cc.25929.
[3] Y., Fu, Delayed Ettringite Formation in Portland cement products, University of Ottawa, 1997.
[4] E.R. Giannini, L.F.M. Sanchez, A. Tuinukuafe, K. j. folliard., Characterization of concrete affected by delayed ettringite formation using the stiffness damage test, Constr. Build. Mater. 162 (2018) 253–264, https://doi.org/10.1016/j.conbuildmat.2017.12.012.
[5] J. Goncalves, M. El-Bakkari, Y. Boluk, V. bindiganavile., Cellulose nanofibres (CNF) for sulphate resistance in cement-based systems, Cem. Concr. Compos. 99 (2019) 100–111, https://doi.org/10.1016/j.cemconcomp.2019.03.005.
[6] S. Chiranjiakumari Devi, R. Ahmad Khan, Influence of graphene oxide on sulfate attack and carbonation of concrete containing recycled concrete aggregate, Constr. Build. Mater. 250 (2020) 118883.
[7] Q. Huang, X. Zhu, L. Zhao, M. Zhao, Y. Liu, X. Zeng, Effect of nanosilica on sulfate resistance of cement mortar under partial immersion, Constr. Build. Mater. 231 (2020), 117180, https://doi.org/10.1016/j.conbuildmat.2019.117180.
[8] R. Gopalakrishnan, R. Jeyalakshmi, The effects on durability and mechanical properties of multiple nano and micro additive OPC mortar exposed to combined chloride and sulfate attack, Mater. Sci. Semicond. Process. 106 (2020), 104772, https://doi.org/10.1016/j.mssp.2019.104772.
[9] C. Nunes, Z. Slížková, M. Stefanidou, J. Němeček, Microstructure of lime and lime-pozzolana pastes with nanosilica, Cem. Concr. Res. 83 (2016) 152–163, https://doi.org/10.1016/j.cemconres.2016.02.004.
[10] G.H. Barbhuiya, M.A. Moiz, S.D. Hasan, M.M. Zaheer, Effects of the nanosilica addition on cement concrete: A review, Mater. Today:. Proc. 32 (2020) 560–566.
[11] E. Horszczaruk, M. Aleksandrzak, K. Cendrowski, R. Jędrzejewski, J. Baranowska, E. Mijowska, Mechanical properties cement-based composites modified with nano-Fe3O4/SiO2, Constr. Build. Mater. 251 (2020) 5–10, https://doi.org/10.1016/j.conbuildmat.2020.118945.
[12] ASTM, **ASTM C 1260:14** - Standard Test Method for Potential Alkali Reactivity of Aggregates (Mortar-Bar Method), (2014).
[13] ABNT, **NBR 15577:18** – Aggregates - Alkali-aggregate reactivity - Part 5: Determination of mitigation of expansion on mortar bars by accelerated mortar-bar method, (2018). [ASTM C1567 Standard Test Method for Determining the Potential Alkali-Silica Reactivity of Combinations of Cementitious Materials and Aggregate (Accelerated Mortar-Bar Method)].
[14] ABNT, **NBR 5739:18** - Concrete - Compression test of cylindrical specimens, (2018). [ASTM C39 Standard Test Method for Compressive Strength of Cylindrical Concrete Specimens].
[15] ABNT, **NBR 8522-1:21.** Hardened concrete - Determination of elasticity and deformation modulus - Part 1: Static modulus by compression (2021). [ASTM C469 Standard Test Method for Static Modulus of Elasticity and Poisson's Ratio of Concrete in Compression].
[16] **Climatologia e histórico de previsão do tempo em Curitiba, PR**. Climatempo. In.: https://www.climatempo.com.br/climatologia/271/curitiba-pr. Access in 17 jan, 2022.
[17] **UNE, 83988-2**. Durabilidad del hormigón – determinación de la resistividad – Parte 2: Método de las cuatro puntas o de Wenner. Associación Española de Normalización y Certificación – AENOR, Madri, Espanha. 2012.
[18] ABNT, **NBR 8802:13**. Hardened concrete - Determination of ultrasonic wave transmission velocity (2013). [EN 12504-4:2021 Testing concrete in structures - Part 4: Determination of ultrasonic pulse velocity].
[19] D.G. Aggelis, E.Z. Kordatos, D.V. Soulioti, T.E. Matikas, Combined use of thermography and ultrasound for the characterization of subsurface cracks in concrete, Elsevier Ltd. Constr. Build. Mater 24 (10) (2010) 1888–1897, https://doi.org/10.1016/j.conbuildmat.2010.04.014.
[20] N. p. hasparyk. Investigação de concretos afetados pela reação álcali-agregado e caracterização avançada do gel exsudado Tese de doutorado. Universidade Federal do Rio Grande do Sul 2005 Porto Alegre, RS 326 Available. In.
[21] N. P. HASPARYK, D. SCHOVANZ, S. C. KUPERMAN, 2020. **INSTRUÇÃO TÉCNICA no GSTE004R0** - Método de Ensaio para a Avaliação do Potencial de Ocorrência da Etringita Tardia (DEF) em Concreto, (2020).
[22] K.F. Portella, N.P. Hasparyk, M.O.G.P. Bragança, J.L. Bronholo, B.G. Dias, L. E. Lagoeiro, Multiple techniques of microstructural characterization of DEF: Case of study with high early strength Portland cement composites, Constr. Build. Mater 311 (2021) 1–13.
[23] H.N. Atahan, D. Dikme, Use of mineral admixtures for enhanced resistance against sulfate attack, Constr. Build. Mater 25 (2011) 3450–3457.
[24] L. Senff, D. Hotza, W.L. Repette, V.M. Ferreira, J.A. Labrincha, Mortars with nano-SiO2 and micro-SiO_2, investigated by experimental design, Constr. Build. Mater 24 (2010) 1432–1437.
[25] X. Brunetaud, L. Divet, D. Damidot, Impact of unrestrained Delayed Ettringite Formation-induced expansion on concrete mechanical properties, Cem. Concr. Res. 38 (2008) 1343–1348.
[26] D. Schovanz, F. Tiecher, N.P. Hasparyk, S.C. Kuperman, R.T. Lermen, Evaluation of Delayed Ettringite Formation through Physical, Mechanical, and Microstructural Assays, ACI Mater. J. 118 (1) (2021) 101–109.
[27] A. Pavoine, X. Brunetaud, L. Divet, The impact of cement parameters on Delayed Ettringite Formation, Cem. Concr. Compos 34 (2012) 521–528.
[28] D. schovanz, Estudo da formação da etringita tardia (DEF) em concretos com cimento Portland pozolânico e de alta resistência, Dissertação de Mestrado. **Faculdade Meridional**, Passo Fundo (2019).
[29] F. Tiecher, M. Langoski, N.P. Hasparyk, Comportamento de argamassas com diferentes tipos de cimento quando induzidas à Formação de Etringita Tardia (DEF), Revista ALCONPAT. 11 (3) (2021) 1–16.
[30] R. SCHMALZ. Durabilidade de argamassas submetidas ao ataque de sulfatos: efeito da adição da nanosílica. Dissertação de Mestrado. **Universidade Federal de São Carlos**, São Carlos, 2018.
[31] S. Zhuang, J. Sun, The feasibility of properly raising temperature for preparing high-volume fly ash or slag steam-cured concrete: An evaluation on DEF, 4-year strength and durability, Constr. Build. Mater. 242 (2020), 118094.
[32] A.S. Silva A.B. Ribeiro L. divet. Prevention of internal sulphate reaction in concrete. Long-term results of the effect of mineral additions 16th ICAAR, International Conference on Alkali-Aggregate Reaction in Concrete, Proceedings 2020–2022. Lisbon.
[33] N.P. Hasparyk, D. Schovanz, F. Tiecher, S.C. Kuperman, Global analysis of DEF damage to concretes with and without fly-ash, Ibracon Structures and Materials Journal 15 (2022) e-15305.
[34] H.F.W. Taylor, C. Famy, K.L. Scrivener, Delayed ettringite formation, Cem. Concr. Res. 31 (5) (2001) 683–693.